BIOENG

Brazilian Journal of Biosystems Engineering (2026), 20 1402

REGULAR ARTICLE

Evaluation of a fuzzy logic–based pH control system: response time and accuracy under simulated fermentation conditions

Junita Tarigan [1]*; Muhammad Atqa Adzkia Zaldi [2]; Umaya Ramadhani Putri Nasution [2]

1 Department of Agricultural and Biosystem Engineering, Universitas Sumatera Utara, Medan, Indonesia

2 Department of Information Technology, Faculty of Computer Science and Information Technology, Universitas Sumatera Utara, Medan, Indonesia

Regular Section

Academic Editor: *Celso Antonio Goulart*

Statements and Declarations

Data availability

The data presented in this study are available on request from the corresponding author.

Institutional Review Board Statement

Not applicable.

Conflicts of interest

The authors declare no conflict of interest.

Funding

This research was fully supported by Universitas Sumatera Utara through the TALENTA USU Research Grant (Contract No. 7248/UN5.2.3.D3/PT.01.03/2025) for the 2025 fiscal year.

Code/Software availability

The control algorithm and source code used in this study are available from the corresponding author upon reasonable request.

Use of Generative AI

Generative AI tools (ChatGPT, OpenAI) were used to assist in language refinement and manuscript editing. All content was reviewed and verified by the authors.

Author contribution (CRediT)

J.T.: Conceptualization, Methodology, Investigation, Data curation, Formal analysis, Writing – original draft, Visualization; M.A.A.Z.: Software, Validation, Formal analysis, Visualization, Writing – review & editing; U.R.P.N.: Conceptualization, Methodology, Supervision, Project administration, Writing – review & editing.

Abstract

pH is a critical parameter in anaerobic fermentation processes, particularly in biohydrogen production, where microbial activity is highly sensitive to environmental conditions. This study aimed to evaluate the performance of a fuzzy logic–based pH control system using standardized buffer solutions to simulate fermentation conditions. The system was developed using an Arduino Uno R4 WiFi microcontroller integrated with a pH sensor, peristaltic dosing pumps, and a mixing unit. Experiments were conducted at laboratory scale with working volumes of 300 mL under acidic (pH 4.5) and alkaline (pH 8.0) initial conditions, targeting an optimal pH range of 5.5–7.0. The pH sensor calibration showed good repeatability but limited accuracy, with a root mean square error (RMSE) of approximately 1.12 pH units. A systematic error pattern was observed, with overestimation in acidic conditions and underestimation in neutral to alkaline ranges, indicating limitations of the linear calibration model. Despite this, the sensor demonstrated stable and consistent measurements. The fuzzy logic control system successfully regulated pH toward the desired set points under both acidic and alkaline conditions. The system exhibited stable and monotonic responses without oscillation or overshoot, demonstrating robust control performance. However, differences in response dynamics were observed: the system responded faster under alkaline conditions than under acidic conditions, reflecting the nonlinear characteristics of the pH scale and mixing dynamics. Overall, the developed system demonstrates the potential of fuzzy logic control for pH regulation in fermentation processes. However, improvements in sensor calibration and response speed, particularly under acidic conditions, are necessary to enhance system accuracy and efficiency.

Keywords

pH control; fuzzy logic control; biohydrogen fermentation; sensor calibration; dynamic response; Arduino-based system

1. Introduction

pH is a critical operational parameter in anaerobic fermentation processes, as it directly influences microbial activity, metabolic pathways, and overall process stability (Sarker et al., 2019). During fermentation, microorganisms actively metabolize organic substrates and produce various intermediate compounds, including organic acids and, in some metabolic stages, alkaline by-products (Nagarajan et al., 2022; de Carvalho & Conte-Junior, 2024). As a consequence, the pH of the fermentation medium may decrease or increase dynamically over time. These pH fluctuations, if not properly controlled, can negatively affect microbial activity and compromise process performance (Gouveia et al., 2017; Ahleboot et al., 2021).

In biohydrogen fermentation systems, maintaining pH within an optimal range is particularly important, since hydrogen-producing bacteria exhibit high sensitivity to acidic or alkaline conditions (Gupta et al., 2024). Deviations from the optimal pH range may reduce hydrogen yield, alter metabolic pathways, or even cause partial or total process inhibition (Moussa et al., 2022). Therefore, effective pH regulation is essential to ensure stable operating conditions and to maximize biohydrogen production efficiency in fermentative biosystems (García-Depraect et al., 2019).

Conventional pH control methods often face limitations when applied to fermentation processes due to their nonlinear behavior, time-varying dynamics, and delayed system responses (Hitit et al., 2026). These challenges have motivated the application of intelligent control approaches capable of handling uncertainty and process variability. Among them, fuzzy logic control has been widely applied in complex engineering systems due to its ability to represent expert knowledge through linguistic rules without requiring an explicit mathematical model. In biosystems engineering applications, fuzzy logic controllers offer flexibility in adapting control actions to changing process conditions (Trabachini et al., 2024).

However, the performance of fuzzy logic–based pH control systems, particularly in terms of response time, accuracy, and stability in achieving a predefined set point, still requires systematic evaluation under controlled conditions. Experimental assessment in real fermentation environments is often affected by biological variability, which may obscure the evaluation of control performance. For this reason, the use of

*Corresponding author

E-mail address: junitatarigan@usu.ac.id

https://doi.org/10.18011/bioeng.2026.v20.1402

Received: 22 April 2026 / Accepted: 30 June 2026 / Available online: 02 July 2026

standardized pH solutions provides a reliable approach to simulate fermentative conditions and enables repeatable and objective testing of control strategies.

Based on this context, the objective of this study was to evaluate the performance of a fuzzy logic–based pH control system using standardized pH solutions as a simulation of anaerobic biohydrogen fermentation conditions, focusing on response dynamics, accuracy, and stability in reaching the desired pH set point.

2. Materials and methods

2.1 Experimental Site and System Overview

The experiment was conducted at a laboratory scale under controlled indoor conditions using a bench-scale fermentation vessel with a working volume of 300 mL. To simulate pH disturbances that may occur during biohydrogen fermentation, test solutions were prepared with initial pH values of 4.5 and 8.0, representing acidic and alkaline conditions outside the desired operating range.

The target pH control range was set between pH 5.5 and 7.0, corresponding to the optimal pH range for biohydrogen-producing microorganisms. The developed pH sensor continuously monitored the solution pH, and the control system automatically activated the dosing pumps whenever the measured pH deviated from the predefined range.

Standard buffer solutions of pH 4.01 and 9.18 were used for sensor calibration prior to each experiment. In addition, the pH 4.01 and pH 9.18 buffer solutions served as the acidic and alkaline dosing solutions supplied by the pumps. When the solution pH exceeded the upper control limit, the acidic buffer solution was injected to reduce the pH. Conversely, when the pH fell below the lower control limit, the alkaline buffer solution was added to increase the pH. This approach enabled the evaluation of the system's ability to restore pH conditions from disturbed states and maintain them within the target operating range.

Although the control system was designed for application in anaerobic biohydrogen fermentation, all experiments were conducted using non-biological test solutions to eliminate the influence of microbial activity and to allow a controlled assessment of sensor accuracy and pH control performance. Each experimental condition was repeated three times to ensure the repeatability and reliability of the results.

The developed system consisted of a pH sensing unit, control unit, actuation unit, and mixing unit. The control algorithm was implemented on an Arduino Uno R4 WiFi microcontroller, which processed real-time pH data and controlled peristaltic dosing pumps via relay modules. Based on the deviation between the measured pH value and the target control range (pH 5.5–7.0), acidic or alkaline solutions were automatically added until the pH returned to and remained within the desired range.

2.2 Materials and Hardware Components

The pH control system was developed using an Arduino Uno R4 WiFi microcontroller as the main control unit. A PH-4502C analog pH sensing module equipped with a BNC-type pH electrode probe was employed to measure the solution acidity in real time. The sensor module was supplied with 5 V, and its analog output was connected to the A0 analog input pin of the microcontroller. During system operation, the analog signal was processed in the firmware as a 0–1023 ADC representation. The corresponding voltage was calculated for monitoring and debugging purposes as V = ADC × 5.0 / 1023.0, while pH estimation was performed using the calibrated ADC-to-pH model.

The actuation system consisted of two 12 V DC peristaltic dosing pumps, designated for acidic and alkaline solution injections, which were controlled through a 5 V three-channel relay module. Based on preliminary measurement, the nominal pump flow rate was approximately 50–51 mL/min. Since the fuzzy controller activated the pumps in short pulses, the effective delivered volume per dosing action may differ from the continuous flow estimate due to pump start-up delay and tubing response. Therefore, pump activation duration was used as the practical control output of the system.

A bench-scale fermentor with a working volume of 1 L was used as the reaction vessel. The fermentor was equipped with a bottom-mounted DC motor operating at 60 RPM, coupled with a mechanical stirrer to homogenize the solution after each dosing action and prevent localized pH gradients. Voltage regulation for the motor and peripheral components was achieved using a DC–DC step-down converter, while dedicated power supply adapters provided stable 5 V and 12 V inputs for the control and actuation units, respectively. Real-time system information was displayed using a 16×2 LCD with an I2C interface.

The overall hardware architecture of the developed monitoring and control system is presented in Figure 1, and the main hardware specifications are summarized in Table 1.

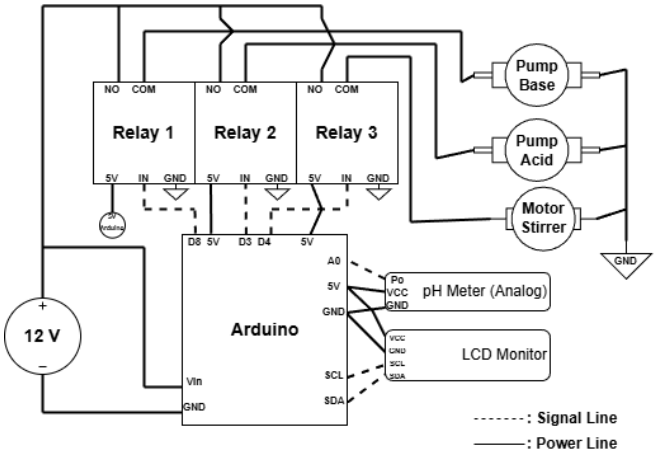

Figure 1. Hardware configuration of the microcontroller-based pH monitoring system.

2.3 pH Sensor Calibration and Accuracy Evaluation

Sensor calibration was performed using a two-point linear calibration approach. The calibration procedure was repeated six times to evaluate measurement consistency and repeatability. The pH values of the calibration solutions were first measured using a reference pH meter, and the measured reference values were entered through the serial monitor during the calibration procedure. Therefore, the calibration was based on the actual reference pH readings rather than only on the nominal values of the prepared buffer solutions.

Table 1. Hardware specifications of the developed pH monitoring and control system.

Component	Specification reported in this study	Function
Microcontroller	Arduino Uno R4	Main control unit for sensing, decision-making, LCD output, and relay actuation
pH sensing module	PH-4502C analog pH module	Analog signal conditioning for pH electrode output
pH probe	BNC-type pH electrode	Measurement of solution acidity/alkalinity
Analog input	A0; firmware-processed ADC representation of 0-1023	ADC acquisition for pH estimation
Dosing pumps	Two 12 V DC peristaltic pumps; nominal flow rate approx. 50-51 mL/min	Separate acid and base dosing
Relay actuation	Relay-based ON-OFF pump control	Electrical isolation and pump switching
Mixing unit	12 V DC motor with mechanical stirrer; approx. 60 RPM	Homogenization after dosing
Display	16 x 2 I2C LCD	Real-time pH and system-status display
Power supply	Dedicated 5 V and 12 V supply rails	Stable supply for control and actuation units

For each calibration point, 50 ADC samples were recorded at 10 ms intervals and averaged to reduce short-term electrical noise. For each trial, ADC values were recorded at two reference pH points, and the corresponding slope and intercept values of the ADC-to-pH model were calculated using Equation (1).

$$pH = aADC + b \quad (1)$$

where a represents the slope and b represents the intercept of the calibration model. Variations in slope and intercept were observed across trials, which were attributed to measurement noise, electrode stabilization time, and environmental factors. To obtain reliable calibration parameters, calibration trials showing substantial deviations from the stable repeated measurement pattern were excluded based on consistency evaluation. Specifically, trials with deviations greater than approximately 5% in ADC readings, slope, or intercept compared with the stable repeated pattern were not used in the final averaged calibration coefficients. Because this exclusion procedure was based on repeated-parameter consistency rather than a formal statistical outlier test, it is reported as a practical consistency-based calibration refinement.

Sensor accuracy was evaluated by comparing the calibrated pH values with reference measurements using error indicators, including root mean square error (RMSE) and coefficient of determination (R^2). The calibration and ADC acquisition procedure is summarized in Table 2.

Table 2. Summary of pH sensor calibration and ADC acquisition procedure.

Calibration item	Implemented procedure
Calibration model	Two-point linear ADC-to-pH calibration: pH = a x ADC + b
Reference pH input	Measured pH values from a reference pH meter entered via serial monitor
Samples per calibration point	50 ADC samples
Sampling interval	10 ms between consecutive samples
Number of calibration trials	Six repeated trials
Trial screening	Practical consistency-based screening; trials with ADC/slope/intercept deviation greater than approximately 5% were excluded
Final coefficients	Average of retained calibration trials
Accuracy evaluation	Comparison with reference pH meter using RMSE and R^2

2.4 Firmware Workflow

To improve the reproducibility of the implemented control procedure, the firmware workflow is presented in Figure 2. The firmware initializes the input/output pins, LCD, serial interface, relay states, and calibration constants. After initialization, the pH sensor signal is acquired through repeated ADC sampling, and the calibrated pH value is calculated using the ADC-to-pH calibration model. The controller then evaluates whether the measured pH is below, within, or above the predefined target control range using the implemented hysteresis logic.

When the measured pH is outside the target range, the firmware calculates the pH deviation from the nearest control boundary and determines the corresponding pump activation duration using the fuzzy inference system. The appropriate dosing pump is then activated according to the detected correction direction: the alkaline pump is activated under low-pH conditions, whereas the acidic pump is activated under high-pH conditions. After each dosing event, the mechanical stirrer is operated, and a fixed 60 s mixing-and-settling delay is applied before the next measurement cycle.

Manual priming commands were included in the firmware to support pump preparation and maintenance. However, the automatic pH regulation sequence was based on the repeated monitoring, fuzzy inference, pump actuation, and mixing cycle shown in Figure 2. Interlocking logic was implemented to ensure that only one dosing pump could be activated during a control cycle, thereby preventing simultaneous acid and base injection. The main firmware and control parameters implemented in the pH regulation system are summarized in Table 3.

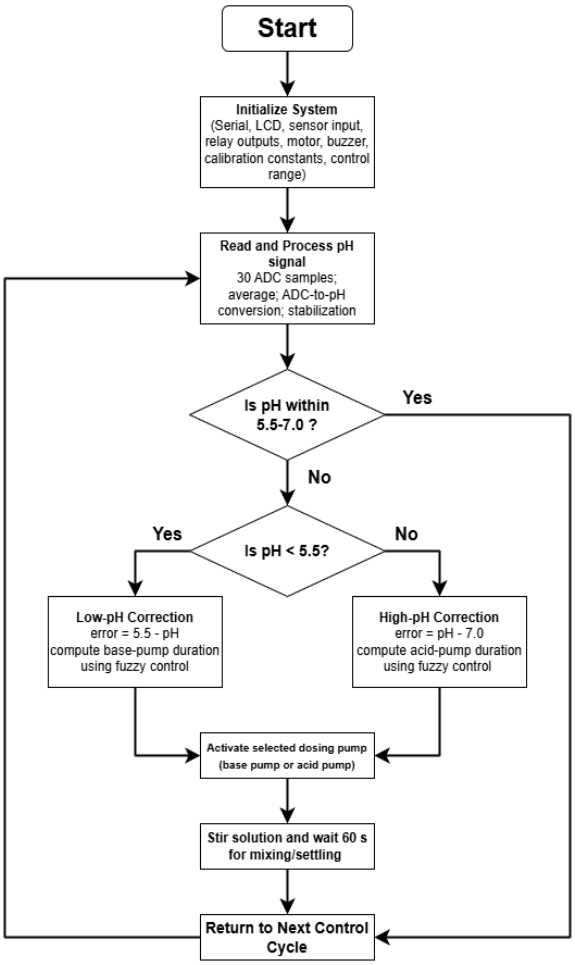

Figure 2. Firmware workflow of the developed pH control system, showing pH signal acquisition, range-based decision-making, fuzzy dosing control, pump actuation, mixing/settling delay, and repeated monitoring cycle.

Table 3. Control system parameter configuration for pH regulation.

Parameter	Value	Function in the control system
Hysteresis band	±0.05 pH units	Prevents rapid switching near the control thresholds
Settling/mixing delay	60 s	Allows solution homogenization before the next pH evaluation
Sample averaging	30 samples per control cycle	Reduces random ADC noise and improves repeatability
Sampling interval	10 ms	Defines the interval between consecutive ADC samples
Filter constant	α = 0.2	Smooths short-term fluctuations while preserving system responsiveness
Pump activation limit	Firmware-defined minimum–maximum pulse duration	Ensures effective dosing while reducing the risk of excessive reagent injection
Fuzzy output upper design limit	2500 ms	Defines the maximum nominal actuation window of the fuzzy controller
Interlocking logic	One pump per control cycle	Prevents simultaneous acid and base injection

2.5 Fuzzy Logic–Based pH Control Strategy

A fuzzy logic control (FLC) algorithm was implemented to regulate the duration of acid or base dosing according to the deviation of the measured pH from the predefined target control range. The controller was designed to maintain the solution pH within the biologically relevant operating window of pH 5.5–7.0. When the measured pH was below the lower boundary, alkaline solution was delivered; when the measured pH exceeded the upper boundary, acidic solution was delivered. This range-based control approach was adopted to correct pH deviations while maintaining stable operating conditions within the desired fermentation window. The fuzzy controller used the magnitude of pH deviation from the nearest control boundary as its input variable. Under low-pH conditions, the input error was calculated as $e = 5.5 - pH$, whereas under high-pH conditions, the input error was calculated as $e = pH - 7.0$. The error value was limited to the designed operating region before fuzzification to avoid excessive actuation under large deviations.

Five linguistic terms were employed to describe the error magnitude, namely very small, small, medium, large, and very large. Each term was represented by a triangular membership function. The fuzzy inference process mapped the input error into a pump activation duration, where larger pH deviations resulted in longer pump activation within the firmware-defined operating limit. The final actuation command was obtained using weighted-average inference. Therefore, the implemented controller can be described as a zero-order Sugeno-type fuzzy inference system, in which each activated rule contributes to the final pump-duration command according to its firing strength. The structure of the fuzzy inference system is shown in Figure 3, while the input membership functions are summarized in Table 4.

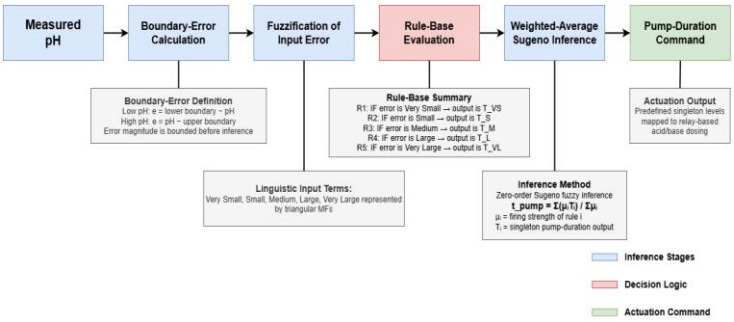

Figure 3. Block diagram of the zero-order Sugeno-type fuzzy inference system used for pump-duration decision support.

Table 4. Input membership functions for pH boundary-error magnitude.

Input term	Triangular MF (a, b, c)	Interpretation
Very small (VS)	(0.0, 0.2, 0.4)	Very small deviation from the control boundary
Small (S)	(0.2, 0.6, 1.0)	Small but actionable deviation
Medium (M)	(0.6, 1.0, 1.4)	Moderate deviation requiring longer dosing
Large (L)	(1.0, 1.4, 1.8)	Large deviation from the target range
Very large (VL)	(1.4, 1.8, 2.2)	Very large deviation approaching the maximum control region

The final pump duration was calculated using the weighted average as shown in Equation (2).

$$t_{pump} = (\Sigma \mu_i T_i)/(\Sigma \mu_i) \quad (2)$$

where t_{pump} is the pump activation duration, μ_i is the membership degree of the i-th input linguistic term, and T_i is the corresponding singleton pump-duration output. In this implementation, the output command was constrained by the firmware-defined pump activation limit, with a maximum nominal actuation window of 2500 ms.

To improve robustness under real measurement conditions, the control algorithm incorporated several signal-conditioning and stability-enhancing features. First, the pH reading for each control cycle was obtained by averaging 30 consecutive ADC samples to reduce random electrical noise and improve repeatability. Second, an exponential smoothing filter with a filter constant of $\alpha = 0.2$ was applied to smooth short-term fluctuations while preserving system responsiveness. Third, a hysteresis band of ±0.05 pH units were implemented around both control boundaries to prevent rapid ON–OFF switching of the pumps due to minor fluctuations near the threshold region.

These features were introduced to improve the reliability and smoothness of the control action under laboratory operating conditions.

2.6 pH Response Testing

For each experiment, the solution was initially adjusted to a pH value outside the predefined target range using standardized buffer solutions representing acidic and alkaline initial conditions. During system operation, the controller continuously processed the measured pH data and evaluated whether the solution was below, within, or above the desired control window. When a deviation from the control range was detected, the appropriate peristaltic pump was activated according to the fuzzy inference output. This control cycle was repeated until the pH returned to and remained within the target range.

After each dosing event, the mechanical stirring motor was operated for a fixed mixing-and-settling period of 60 s before the subsequent pH evaluation. This delay was introduced to allow adequate homogenization of the solution and to avoid inaccurate control decisions caused by temporary local concentration gradients immediately after reagent addition. The use of a defined settling period also contributed to smoother control behavior and reduced the likelihood of overshoot due to premature re-measurement.

System performance was evaluated based on the ability of the controller to restore the pH toward the desired operating region and maintain stable behavior thereafter. Particular attention was given to the response time, monotonicity of correction, stability near the target region, and the presence or absence of oscillation and overshoot under both acidic and alkaline initial conditions.

This procedure enabled the dynamic characteristics of the fuzzy logic–based pH control system to be assessed under repeatable simulated fermentative conditions. The experimental setup used for evaluating the automated pH control system is illustrated in Figure 4.

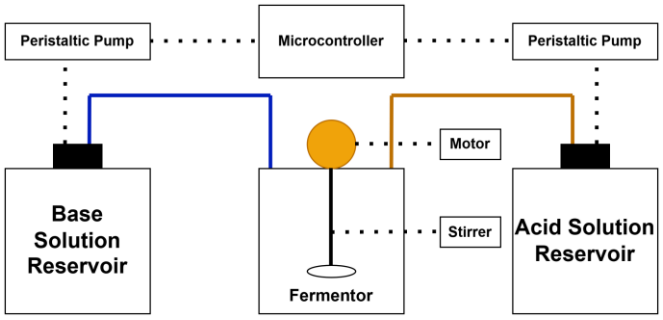

Figure 4. Experimental Setup of the Automated pH Control System.

3. Results and discussion

3.1 pH Sensor Calibration and Accuracy

The performance of the developed pH sensor was evaluated by comparing its readings with those obtained from a laboratory-grade reference pH meter across a wide measurement range (pH 2.32–12.42). The relationship between actual and measured pH values is illustrated in Figure 5.

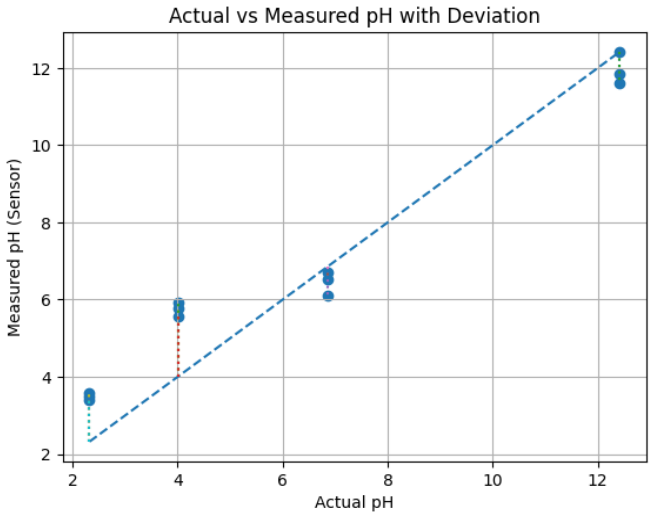

Figure 5. The relationship between actual and measured pH.

The graphical comparison shows that the measured values deviate from the ideal linear response, represented by the dashed line (y = x). The deviation is visually emphasized by vertical lines, which indicate the magnitude of measurement error for each data point. Quantitatively, the sensor exhibited a root mean square error (RMSE) of approximately 1.12 pH units, indicating a relatively high deviation from the reference measurements. Similar approaches using RMSE as a primary indicator of sensor accuracy are widely adopted in electrochemical sensor evaluation studies (Baranwal et al., 2022). The obtained RMSE value of approximately 1.12 pH units indicates that the developed sensor still exhibits considerable deviation from reference measurements, particularly under extreme acidic conditions. In practical fermentation systems, such an error may influence the accuracy of automatic dosing decisions, since microbial activity in biohydrogen fermentation is highly sensitive to pH fluctuations. For example, deviations beyond the optimal pH range may alter metabolic pathways and reduce hydrogen production efficiency.

The pH control system exhibited a faster response under alkaline conditions than under acidic conditions. The average settling time was 15.67 ± 1.15 min under alkaline conditions and 31.33 ± 14.50 min under acidic conditions. The steady state errors were relatively low, reaching 0.02 and 0.04 pH units for acidic and alkaline conditions, respectively. Dynamic Performance Parameters of the pH Control System Under Acidic and Alkaline Conditions are presented in Table 5.

Table 5. Dynamic Performance Parameters of the pH Control System Under Acidic and Alkaline Conditions.

Parameter	Acidic Condition	Alkaline Condition
Set Point (pH)	5.50	7.00
Tolerance Band (± pH)	0.05	0.05
Rise Time, Tr (min)	23	7.00
Settling Time, Ts (min)	31.33 ± 14.50	15.67 ± 1.15
Steady-State pH	5.48	7.04
Steady-State Error, Ess (pH unit)	0.02	0.04

Nevertheless, the acceptability of this error depends on the intended application of the system. For preliminary laboratory-scale monitoring and proof-of-concept control studies, the observed RMSE may still be acceptable because the control objective in this study was maintaining the pH within a relatively broad operational window (pH 5.5–7.0) rather than achieving highly precise analytical measurements. Furthermore, the system demonstrated stable and repeatable responses despite systematic bias. However, for industrial-scale bioprocesses or applications requiring strict pH regulation, further calibration refinement and higher-accuracy sensing methods would be necessary to minimize control error and improve process reliability.

A clear pattern of systematic error is observed from the experimental results. In the acidic region (pH 2.32–4.01), the sensor consistently overestimates the pH value, with deviations reaching up to +1.74 pH units. In contrast, in the neutral to alkaline range (pH 6.86–12.42), the sensor tends to underestimate the pH, although with smaller deviations (approximately ±0.5 pH units). This asymmetric error distribution indicates that the sensor does not follow a perfectly linear response across the entire pH range. Such behavior is commonly reported in low-cost pH sensing systems, where electrode response and signal conditioning introduce non-linearities, particularly at extreme pH levels (Cheng & Zhu, 2005; Shylendra et al., 2021).

Despite the observed inaccuracies, the sensor demonstrates good repeatability. Measurements taken at the same pH level show relatively low variation, typically within ±0.2–0.3 pH units. This indicates that the sensor produces stable and consistent readings under identical conditions. This distinction highlights that the system exhibits high precision but limited accuracy, a condition often associated with systematic calibration errors rather than random noise. In electrochemical sensing, such behavior typically suggests that the measurement system is stable, but the calibration model does not adequately represent the true sensor characteristics.

The calibration of the sensor was performed using a linear regression model that relates ADC values to pH. While this approach is simple and widely used, it assumes a constant sensitivity across the entire measurement range. However, the electrochemical behavior of pH electrodes is governed by the Nernst equation (Rocha et al., 2026). Under ideal conditions, the electrode exhibits a slope of approximately 59.16 mV/pH at 25°C. However, practical implementations often deviate from this ideal behavior due to electrode aging, temperature variation, and imperfect calibration (Zhang et al., 2025).

The significant deviation observed in the acidic region suggests that the linear calibration model is insufficient to capture the true sensor response over a wide pH range. Previous studies have shown that non-linear calibration methods, such as polynomial regression, can significantly improve accuracy in similar sensing systems (Berger et al., 2019; Jamil et al., 2023; Mohamed et al., 2023).

The observed accuracy characteristics have important implications for real-world applications. The relatively good performance in the neutral to alkaline range suggests that the sensor is suitable for applications such as water quality monitoring and agricultural systems, where extreme pH conditions are less frequent.

However, the large deviation in acidic conditions may limit its applicability in processes requiring high accuracy at low pH levels, such as fermentation and chemical processing. Furthermore, for control systems such as fuzzy logic-based pH regulation the presence of systematic bias may lead to incorrect control actions, particularly in extreme conditions. This can result in instability or overshoot in closed-loop control systems. These findings are consistent with previously reported limitations of low-cost electrochemical pH sensing systems (Zeta et al., 2025; Fratz-Berilla et al., 2024) and highlight the importance of advanced calibration strategies to improve measurement performance.

3.2 Dynamic Response of the Fuzzy Logic Control System

The performance of the pH control system was evaluated under both acidic and alkaline initial conditions. In the acidic case (300 mL solution), the system regulated the pH from approximately 4.9 toward a set point of 5.5, while in the alkaline case, the system reduced the pH from approximately 8 toward a neutral set point (pH 7). The dynamic response of the control system under alkaline and acidic conditions is presented in Figures 6 and 7, respectively.

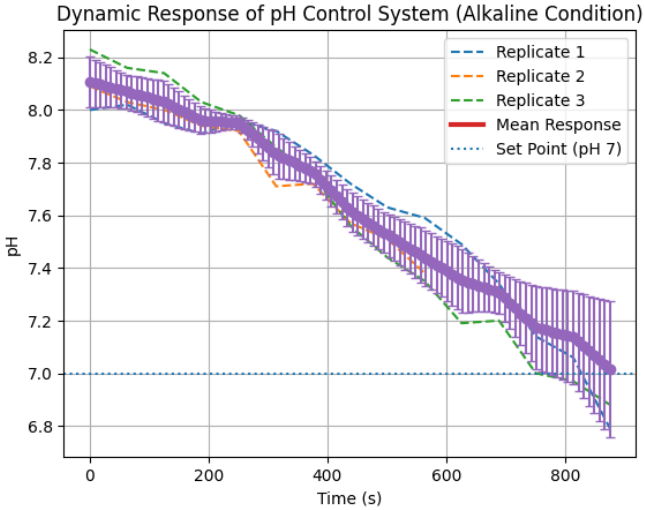

Figure 6. Dynamic Response of pH Control System (Alkaline Condition).

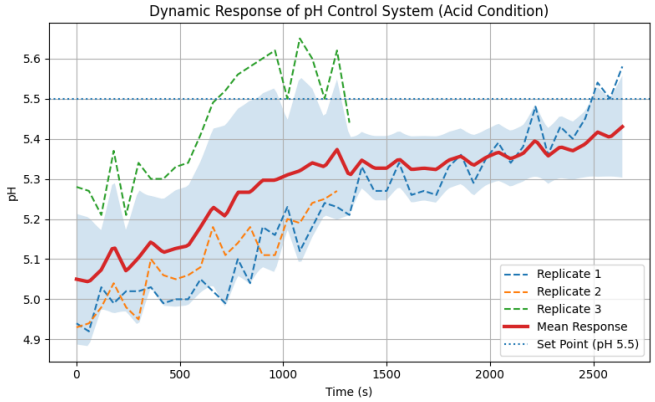

Figure 7. Dynamic Response of pH Control System (Acid Condition).

3.3 Dynamic behavior between acidic and alkaline conditions

Under acidic conditions, the system exhibited a gradual increase in pH from approximately 4.9 to 5.5. The response was relatively slow and smooth, with no indication of oscillation or instability. The control system maintained a continuous dosing action (pump activation) until the set point was reached, after which the system transitioned to a stable "OK" condition.

The response trend suggests that the system operates conservatively, prioritizing stability over speed. This is evident from the small incremental changes in pH and the relatively long time required to reach steady-state conditions. In contrast, under alkaline conditions, the system demonstrated a decreasing pH trend toward the neutral set point (pH 7). The response was also stable and monotonic, but relatively faster compared to the acidic case. The system showed efficient correction without significant overshoot, indicating effective control of acid dosing.

A clear difference in dynamic response can be observed between the two conditions. The acidic adjustment (pH 4.9 to 5.5) required a longer time and exhibited slower convergence compared to the alkaline adjustment (pH 8 to 7). This indicates that the system responds more efficiently when reducing pH (alkaline case) than when increasing pH (acidic case). A comparative analysis of the control responses under acidic and alkaline conditions is shown in Figure 8.

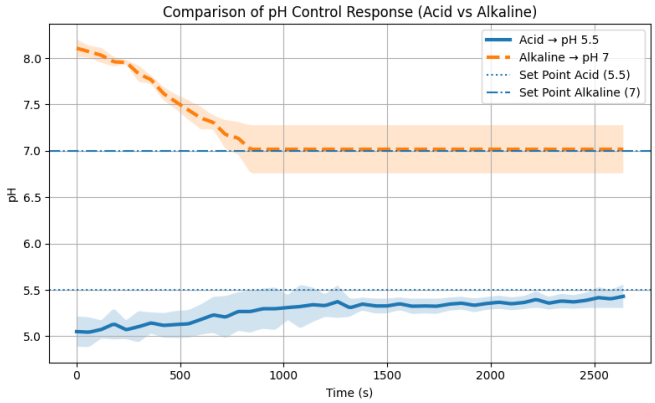

Figure 8. Comparison of pH Control Response (Acid vs Alkaline).

This asymmetric behavior can be explained by the nonlinear and logarithmic nature of the pH scale. Near the acidic region, changes in hydrogen ion concentration produce smaller variations in pH compared to regions near neutrality or alkalinity. As a result, increasing pH in acidic conditions requires more control effort and time. Additionally, mixing dynamics and reagent effectiveness may contribute to the slower response, as base addition in acidic solutions may exhibit delayed homogenization compared to acid addition in alkaline conditions.

Despite the difference in response time, both conditions demonstrate stable control performance. The absence of oscillation and overshoot in both cases indicates that the control algorithm is robust and capable of handling nonlinear system behavior. The consistent response across replicates further confirms the reliability of the system.

Overall, the pH control system successfully regulates both acidic and alkaline conditions toward their respective set points. However, the response speed differs significantly, with faster convergence observed in alkaline conditions. This highlights the importance of considering process nonlinearity in control system design and suggests that further optimization may be required to improve response time in acidic conditions.

3.4 Limitations of Simulated Fermentation Conditions

Although standardized buffer solutions provide highly controlled and repeatable experimental conditions, they do not fully represent the complexity of real fermentation media. In actual anaerobic fermentation systems, the medium contains microorganisms, suspended solids, dissolved organic compounds, metabolic intermediates, and dynamically changing chemical compositions that may significantly affect pH behavior and control performance (Tarigan & Furqon, 2026).

One important difference is the presence of biological variability. Microbial metabolic activity continuously produces acidic and alkaline compounds during fermentation, causing unpredictable and time-varying pH fluctuations (Gouveia et al., 2017). Such behavior cannot be fully replicated using static buffer solutions. The complexity of actual fermentation broth may also influence sensor performance through electrode fouling, signal drift, gas formation, and mixing heterogeneity. Therefore, although the present study successfully demonstrates the feasibility of fuzzy logic–based pH regulation under controlled laboratory conditions, further validation using real fermentation systems is required before practical implementation.

3.5 Scalability and Future Development

The developed fuzzy logic–based pH control system demonstrates potential for implementation in larger-scale fermentation processes and industrial bioreactor systems. The use of low-cost microcontrollers, modular sensors, and peristaltic dosing pumps provide flexibility for scaling the system architecture according to process capacity requirements. However, several challenges must be addressed before industrial implementation can be achieved. Larger fermentation volumes generally exhibit slower mixing dynamics, higher buffering capacity, and more complex spatial pH distributions, which may reduce control responsiveness and increase stabilization time. In addition, industrial fermentation systems often involve continuously changing biological activity and process disturbances that require more adaptive control strategies.

Future developments may include the integration of higher-accuracy industrial-grade pH sensors, adaptive fuzzy logic algorithms, automatic self-calibration mechanisms, and real-time data logging systems. The incorporation of Internet of Things (IoT)-based monitoring and supervisory control systems may also improve process automation and operational reliability in large-scale applications.

4. Conclusions

This study aimed to evaluate the performance of a fuzzy logic–based pH control system in terms of response time, accuracy, and stability in achieving the desired set point under simulated fermentative conditions. The results showed that the system was able to regulate pH from approximately 4.9 to 5.5 (acidic condition) and from 8.0 to 7.0 (alkaline condition) within the target control range of 5.5–7.0. The control response was stable and monotonic in both conditions, with no oscillation or overshoot observed.

In terms of accuracy, the pH sensor exhibited good repeatability (±0.2–0.3 pH units) but limited accuracy, with a root mean square error (RMSE) of approximately 1.12 pH units. A systematic error pattern was observed, including overestimation in acidic conditions (up to +1.74 pH units) and underestimation in neutral to alkaline conditions (approximately ±0.5 pH units). Regarding response characteristics, the system demonstrated faster response under alkaline conditions compared to acidic conditions, indicating differences in dynamic behavior depending on the initial pH.

Acknowledgements

The authors would like to thank the Laboratory of Agricultural Engineering, Universitas Sumatera Utara, for providing facilities and technical support.

References

Ahleboot, Z., Khorshidtalab, M., Motahari, P., Mahboudi, R., Arjmand, R., Mokarizadeh, A., & Maleknia, S. (2021). Designing a strategy for pH control to improve CHO cell productivity in bioreactor. Avicenna Journal of Medical Biotechnology, 13(3), 123–130. https://doi.org/10.18502/ajmb.v13i3.6365

Baranwal, J., Barse, B., Gatto, G., Broncová, G., & Kumar, A. (2022). Electrochemical sensors and their applications: A review. Chemosensors, 10(9), 363. https://doi.org/10.3390/chemosensors10090363

Berger, M., Huber, S., Schott, C., & Paul, O. (2019). Half-Blind Calibration for the Efficient Compensation of Parasitic Cross-Sensitivities in Nonlinear Multisensor Systems. IEEE Sensors Journal, 19, 7005–7014. https://doi.org/10.1109/jsen.2019.2913567

Cheng, K. L., & Zhu, D.-M. (2005). On calibration of pH meters. Sensors, 5(4), 209–219. https://doi.org/10.3390/s5040209

de Carvalho, A. P. A., & Conte-Junior, C. A. (2024). Health and bioactive compounds of fermented foods and by-products. Fermentation, 10(1), 13. https://doi.org/10.3390/fermentation10010013

Fratz-Berilla, E., Kohnhorst, C., Trunfio, N., Bush, X., Gyorgypal, A., & Agarabi, C. (2024). Evaluation of single-use optical and electrochemical pH sensors in upstream bioprocessing. Heliyon, 10, e25512. https://doi.org/10.1016/j.heliyon.2024.e25512

García-Depraect, O., Rene, E. R., Gómez-Romero, J., López-López, A., & León-Becerril, E. (2019). Enhanced biohydrogen production from the dark co-fermentation of tequila vinasse and nixtamalization wastewater: Novel insights into ecological regulation by pH. Fuel, 253, 159–166. https://doi.org/10.1016/j.fuel.2019.04.147

Gouveia, A. R., Freitas, E. B., Galinha, C. F., Carvalho, G., Duque, A., & Reis, M. (2017). Dynamic change of pH in acidogenic fermentation of cheese whey towards polyhydroxyalkanoates production: Impact on performance and microbial population. New Biotechnology, 37, 108–116. https://doi.org/10.1016/j.nbt.2016.07.001

Gupta, S., Fernandes, A., Lopes, A., Grasa, L., & Salafranca, J. (2024). Review: Microbes and parameters influencing dark fermentation for hydrogen production. Applied Sciences, 14(23), 10789. https://doi.org/10.3390/app142310789

Hitit, Z. Y., Demirtaş, G., & Akay, B. (2026). Enhancing pH control in a bioreactor through experimental system identification and dynamic analysis. Chemical Industry & Chemical Engineering Quarterly. Advance online publication. https://doi.org/10.2298/CICEQ250610032H

Jamil, A., Ting, T. S., Abidin, Z. Z., Othman, M., Wahab, M. H. A., Abdullah, M. F. L., Homam, M. J., Audah, L. H. M., & Shah, S. M. (2023). Polynomial regression calibration method of total dissolved solids sensor for hydroponic systems. Pertanika Journal of Science & Technology, 31(6). https://doi.org/10.47836/pjst.31.6.08

Mohamed, H., Nava, G., Vanteddu, P., Braghin, F., & Pucci, D. (2023). Nonlinear in-situ calibration of strain-gauge force/torque sensors for humanoid robots. In Proceedings of the 2023 IEEE-RAS 22nd International Conference on Humanoid Robots (Humanoids) (pp. 1–8). https://doi.org/10.1109/humanoids57100.2023.10375227

Moussa, R. N., Moussa, N., & Dionisi, D. (2022). Hydrogen production from biomass and organic waste using dark fermentation: An analysis of literature data on the effect of operating parameters on process performance. Processes, 10(1), 156. https://doi.org/10.3390/pr10010156

Nagarajan, M., Rajasekaran, B., & Venkatachalam, K. (2022). Microbial metabolites in fermented food products and their potential benefits. International Food Research Journal, 29(3), 466–486. https://doi.org/10.47836/ifrj.29.3.01

Rocha, R. G., Marra, M. C., Richter, E. M., & Muñoz, R. A. A. (2026). Anodization treatment of flexible graphite sheet electrodes for Nernstian pH sensing. Talanta, 297, 128677. https://doi.org/10.1016/j.talanta.2025.128677

Sarker, S., Lamb, J. J., Hjelme, D. R., & Lien, K. M. (2019). A review of the role of critical parameters in the design and operation of biogas production plants. Applied Sciences, 9(9), 1915. https://doi.org/10.3390/app9091915

Shylendra, S. P., Lonsdale, W., Wajrak, M., Nur-E-Alam, M., & Alameh, K. (2021). Titanium nitride thin film based low-redox-interference potentiometric pH sensing electrodes. Sensors, 21(1), 42. https://doi.org/10.3390/s21010042

Tarigan, J., & Furqon. (2026). Effect of co-substrate ratio on pH, redox potential, and cumulative gas from pineapple pulp residue and cow manure. IOP Conference Series: Earth and Environmental Science, 1583(1), 012035. https://doi.org/10.1088/1755-1315/1583/1/012035

Trabachini, A., Dias, C. S., Moreira, M. R., Wen, T. C., Caneppele, F., Harada, É., Amorim, M. N., & Miranda, K. O. S. (2024). Automation to improve pig welfare using fuzzy logic. Revista Brasileira de Ciências Agrárias, 19(3), e3532

Zeta, B. M. A., Alam, S. U., Rahman, G. M. A. E. U., & Ahmed, K. I. U. (2025). A low-cost pH sensor for real-time monitoring of aquaculture systems in a multi-layer wireless sensor network. Sensors, 25(9), 2824. https://doi.org/10.3390/s25092824

Zhang, L., Zhao, D., Tang, W., Chen, Y., & Huang, J. (2025). Proton-relaying adsorbates induce non-Nernstian behavior in oxygen reduction. ACS Catalysis, 15, 14191–14206. https://doi.org/10.1021/acscatal.5c01767